

Supporting Information

In vitro cytotoxicity of Mn(I) and Ru(II) carbonyls with diphenyl pyridyl phosphine
coligand towards Leukaemia

Ahmed M. Mansour,^{*a} Rabaa M. Khaled,^a Krzysztof Radacki,^b Zeina Younes,^c Mariam
Gamal,^c Beatrice Guirguis,^c Gamal A. E. Mostafa,^d Essam A. Ali,^d and Ola R. Shehab^a

^a *Department of Chemistry, Faculty of Science, Cairo University, Gamma Street, Giza, Cairo 12613, Egypt. E-mail: mansour@sci.cu.edu.eg; inorganic_am@yahoo.com*

^b *Institut für Anorganische Chemie, Julius-Maximilians-Universität Würzburg, Am Hubland, D-97074 Würzburg, Germany.*

^c *Department of Biotechnology, Faculty of Science, Cairo University, Gamma Street, Giza, Cairo 12613, Egypt.*

^d *Department of Pharmaceutical Chemistry, College of Pharmacy, King Saud University, Riyadh 11451, Saudi Arabia.*

Section A: Experimental

Section B: Supplementary figures

Section A: Experimental

1. Materials and instruments

Bromo penta-carbonyl manganese(I), diphenyl-2-pyridylphosphine, and organic solvents were acquired from commercial resources and used as received. $[\text{RuCl}_2(\text{CO})_2]_n$,¹ was synthesized following the published procedure using hydrated RuCl_3 , *para*-formaldehyde, and ultra-pure formic acid. The ^1H NMR resonances of Mn(I) (**1**) and Ru(II) (**2**) complexes were recorded on a Bruker-Advance 400 MHz spectrometer. Solvatochromism and CO releasing kinetics were examined using a Specord 210 Plus spectrophotometer. IR spectra of the complexes were recorded using JASCO FT/IR-4100 instrument. The Vario EL III Elementar automatic CHNS analyzer was used to obtain the micro elemental analyses. An Advion compact mass spectrometer was used to record the positive mode electrospray ionization mass spectra.

2. Synthesis of metal carbonyls complexes

$[\text{MnBr}(\text{CO})_2(\kappa^1\text{-P-PPh}_2\text{Py})(\kappa^2\text{-P-N-PPh}_2\text{Py})]$ (**1**): To a flat-bottomed flask charged with diphenyl-2-pyridylphosphine (PPh_2Py) (0.72 mmol; 189 mg) and $[\text{MnBr}(\text{CO})_5]$ (0.36 mmol; 100 mg), acetone (15 mL) was added. Under the dark conditions, the flask was heated to reflux for 6 h. Upon cooling, a reddish-brown precipitate developed. The precipitate was collected, washed with *n*-hexane, and then dried under vacuum. IR (ATR): $\nu = 3051, 2040$ (w, $\text{C}\equiv\text{O}$), 1953 (vs, $\text{C}\equiv\text{O}$), 1898 (vs, $\text{C}\equiv\text{O}$), 1567, 1432, 1088, 744, 630, 515 cm^{-1} . ^1H NMR (400.40 MHz, CDCl_3): $\delta = 8.88$ (br, 1H), 7.94 (br, 4H), 7.43 (br, 9H) ppm. Because of the quadrupolar nuclear and long relaxation time, it was difficult to ascribe ^1H NMR signals of **1**.² ESI-MS (positive mode, acetone): $m/z = 635.31$ ($\text{M}-\text{Br}$)⁺ ($\text{M} = \text{molecular formula}$). $\text{C}_{37}\text{H}_{28}\text{BrMnN}_2\text{O}_3\text{P}_2$: C 59.62, H 3.79, N 3.76; found C 59.47, H 3.43, N 3.44. $[\text{RuCl}_2(\text{CO})(\kappa^1\text{-P-PPh}_2\text{Py})(\kappa^2\text{-P-N-PPh}_2\text{Py})]$ (**2**): To a round-bottomed flask charged with $[\text{RuCl}(\mu\text{-Cl})(\text{CO})_3]_2$ (87 mg, 0.17 mmol), was added methanol (20 mL). The mixture was heated to reflux for 3 h. To the clear orange solution was then added 0.68 mmol of PPh_2Py (178 mg) and refluxing was continued for 24 h. Yellow powder formed upon the evaporation of the reaction solvent, washed with diethyl ether (3 x 5 mL) and dried under vacuum. IR (ATR): $\nu = 3053, 1968$ (vs, $\text{C}\equiv\text{O}$), 1566, 1481, 1433, 1090, 748, 693, 582, 515 cm^{-1} . ^1H NMR (400.40 MHz, DMSO-d_6): $\delta = 8.80$ (br, 1H), 8.50 (d, $^3J_{\text{H,H}} = 5.01$ Hz, 1H), 8.17 (t, $^3J_{\text{H,H}} = 8.68$ Hz, 1H), 7.91–7.19 (m, 24H), 7.10 (m, 1H) ppm. ESI-MS (positive mode, DMSO/acetone): $m/z = 691.26$ $[\text{RuCl}(\text{CO})(\kappa^1\text{-P-PPh}_2\text{Py})(\kappa^2\text{-P-N-}$

PPh₂Py)]⁺. C₃₇H₂₈BrMnN₂O₃P₂: C 59.62, H 3.79, N 3.76; found C 59.47, H 3.43, N 3.44. C₃₆H₂₈Cl₂N₂O₂P₂Ru: C 57.30, H 3.74, N 3.71; found C 57.35, H 3.26, N 3.56.

3. Single crystal X-ray diffraction analysis

Over the course of two weeks, the solutions of **2** and **1a** (iCORM of complex **1**), in chloroform, slowly evaporated in presence of n-hexane, yielding single crystals appropriate for X-ray crystallography. Using a RIGAKU XtaLAB Synergy-R diffractometer equipped with a semiconductor HPA-detector (HyPix-6000) and multi-layer mirror monochromated Cu-K radiation, the diffraction data of **2** were collected at 100 K. The intrinsic phasing approach (SHELXT programme) was used to solve the structures of **2** and **1a**,³ which was then improved using the SHELXL programme and the SHELXLE graphical user interface.⁴ The free pyridyl arm of the monodentate PPh₂Py ligand (κ^1 -P-PPh₂Py mode) in **2** was disordered between two positions (position assigned based on U_{iso} of ortho-atom and presence of residual density of hydrogen atom on this position). The displacement parameters of disordered atoms C2 and N2 of these two residues were constrained to the same value with EADP keyword. The distances between atoms C1–N2 and N2–C3 and C1–C2 and C2–C3 were respectively constrained to the same value during refinement. Crystal data for **2**: C₃₅H₂₈Cl₂N₂OP₂Ru, $M_r = 726.50$, orange block, 0.250 × 0.200 × 0.180 mm³, monoclinic space group $P2_1/n$, $a = 11.37234(9)$ Å, $b = 10.76781(8)$ Å, $c = 25.48891(16)$ Å, $\alpha = 90^\circ$, $\beta = 93.5906(7)^\circ$, $\gamma = 90^\circ$, $V = 3115.12(4)$ Å³, $Z = 4$, $r_{calcd} = 1.549$ g·cm⁻³, $\mu = 6.877$ mm⁻¹, $F(000) = 1472$, $T = 100(2)$ K, $R_1 = 0.0306$, $wR_2 = 0.0768$, 6332 independent reflections [$2\theta \leq 150.228^\circ$] and 395 parameters. In the case of **1a**, the displacement parameters of disordered and overlapping atoms Br1 and Cl1 (Br was probably exchange with Cl during crystallization from chloroform) were constrained to the same value with EADP keyword. Crystal data for **1a**: C₃₄H₂₈Br_{1.30}Cl_{0.70}MnN₂O₂P₂, $M_r = 742.34$, clear yellow block, 0.160 × 0.110 × 0.090 mm³, monoclinic space group $C2/c$, $a = 21.9592(3)$ Å, $b = 11.30260(10)$ Å, $c = 13.1315(2)$ Å, $\beta = 101.6700(10)^\circ$, $V = 3191.81(7)$ Å³, $Z = 4$, $r_{calcd} = 1.545$ g·cm⁻³, $\mu = 7.033$ mm⁻¹, $F(000) = 1498$, $T = 100(2)$ K, $R_1 = 0.0218$, $wR_2 = 0.0545$, 3210 independent reflections [$2\theta \leq 150.304^\circ$] and 199 parameters. Crystallographic data have been deposited with the Cambridge Crystallographic Data Center as supplementary publication no. CCDC-2267579 (**1a**) and CCDC-2267580 (**2**). These data can be obtained free of charge from The Cambridge Crystallographic Data Centre via www.ccdc.cam.ac.uk/data_request/cif

4. DFT/TDDFT calculations

Full geometry optimization of **1** and **2**, in the ground state, was performed using a Becke 3-parameter (exchange) Lee–Yang–Parr functional^{5, 6} and LANL2DZ basis set.^{7, 8} Based on its crystallographic data, the beginning coordinates for optimizing **2** were established. The local minimum structures of **1** and **2** were validated as minimum on the potential energy surface by computing vibrational modes. There were no phantom vibrations here. Time-dependent density functional theory calculations were done using the B3LYP/LANL2DZ computational method as well as the polarizable continuum model (PCM) solvation model. All calculations were carried out using Gaussian03.⁹ Visualization of the electronic spectra and frontier molecular orbitals was achieved using Gaussview03.¹⁰

5. Myoglobin assay

The number of CO equivalents released from PhotoCORM **1** was spectrophotometrically measured by myoglobin (Mb) assay while observing the transformation of Mb into Mb-CO species.^{11, 12} In a quartz cuvette, a buffered solution of standardised horse skeletal muscle myoglobin (Sigma-Aldrich) (0.1 M phosphate-buffered saline, pH = 7.4, 870 μ L) was reduced by adding 200 μ L sodium dithionite solution. Next, 10 μ L of the PhotoCORMs, dissolved in DMSO, was added to complete the volume (1 mL) of the quartz cuvette. The stock solution concentrations were chosen to yield a final mixture of 10 mM dithionite, 60 μ M myoglobin, and 10 μ M CORM. In the case of **1**, 468 nm custom-built LED light source was used for illumination (Kingbright Elec. Co., 5000 mcd, part. no. BL0106-15-299). The photo flow of the light source (1.25×10^{-9} Einstein s^{-1}) was determined using the ferrioxalate actinometry test. For complex **2**, portable UV/Vis hand lamp (365 nm, UVlite LF-206LS, 6 W, UVlite Ltd, Cambridge, UK) was applied. The sealed cuvette was positioned 3 cm from the lamp, and illumination was intermittently disrupted to collect UV/Vis spectra on a Specord 210 Plus spectrophotometer until no longer any changes in the Q-band region were observed. Data was evaluated as described previously.^{11, 12}

6. Biological activity

6.1. Cells

Human acute monocytic leukaemia (THP-1), was obtained from ATCC, USA. The healthy mice bone marrow stromal cells (BM) were prepared using the protocol developed by Maridas and co-workers with slight modifications.¹³

6.2. Cell cultures

All used cell lines were cultured using the RPMI-1640 medium. The medium was supplemented with 10% fetal bovine serum (FBS), 2 mM L-glutamine, containing 100 units/ml penicillin G sodium, 100 units/ml streptomycin sulfate, and 250 ng/ml amphotericin B. All the reagents were obtained from Lonza (Basel, Switzerland). Cells were preserved at sub-confluency in humidified air with 5% CO₂ at 37 °C. When cells confluency had reached 75%, they were utilized after trypsin/EDTA treatment at 37 °C.

6.3. MTT assay

3-[4,5-dimethylthiazole-2-yl]-2,5-diphenyltetrazolium bromide (MTT) was purchased from Merck KGaA (Darmstadt, Germany). The potency of the free ligand, Diphenyl-2-pyridylphosphine and complexes (**1** and **2**) was examined, with and without the illumination at 468 nm, against the malignant and healthy cell lines. The MTT assay is based on the fact that the dark blue, insoluble formazan crystals are produced when the active mitochondrial dehydrogenase enzyme of living cells cleaves the tetrazolium rings of the yellow MTT. When the formazan crystals are dissolved, a dark blue colour that is directly correlated with the quantity of living cells is released. Two plates were prepared and treated with the same compound at the same concentration; one was left in the dark, while the other received 468 nm LED illumination for two hours right after the addition of the test compounds. The two plates were incubated in the dark for total 24 h. Briefly, cells (1×10^4 cells/well) were seeded in serum-free media in a flat bottom 96-well microplate and treated with 20 μ l of serial dilutions of the tested substances starting at 100 μ g/mL and ending at 3.125 μ g/mL after being planted in the relevant media of each cell line at 37° C, in a humidified 5% CO₂ atmosphere. This was followed by an additional 4 h of incubation.

For adherent cells, 180 μ l of acidified isopropanol/well was added, while for suspended cells, 100 μ l of sodium dodecyl sulphate (SDS) was added. After complete solubilization, the photometric determination of the absorbance at 570 nm using a microplate ELISA reader (FLUOstar OPTIMA, BMG LABTECH GmbH, Ortenberg, Germany) was done. Three times repeats were performed for each concentration and the average was calculated.¹⁴

Figure S1	IR spectra of a) [MnBr(CO) ₂ (κ ¹ -P-PPh ₂ Py)(κ ² -P-N-PPh ₂ Py)] (1) and b) [RuCl ₂ (CO)(κ ¹ -P-PPh ₂ Py)(κ ² -P-N-PPh ₂ Py)] (2).	S8
Figure S2	¹ H NMR spectrum (in CD ₃ Cl ₃) of complex 1 .	S9
Figure S3	¹ H NMR spectrum (in DMSO-d ₆) of complex 2 .	S9
Table S1	Single-crystal X-ray diffraction data of complex 2 .	S10
Figure 4	The electronic absorption spectra of 1 in a) DMSO (0.53 mM) and b) 50% DMSO/water mixture (0.17 mM).	S11
Figure S5	The electronic absorption spectra of 1 in different solvents showing solvatochromic behaviour.	S12
Table S2	The absorbance maxima (λ _{max} , nm) and molar extinction coefficient of the lowest energy transition of 1 in different solvents.	S13
Figure S6	The electronic absorption spectra of 2 in a) DMSO (0.13 mM) and b) 75% DMSO/water mixture (0.20 mM).	S14
Figure S7	TDDFT calculated absorption spectra of a) 1 and b) 2 , obtained at B3LYP/LANL2DZ level of theory	S15
Figure S8	Selected electronic transitions and Frontier molecular orbitals of complex 2 , calculated at B3LYP/LANL2DZ level of theory.	S16
Figure S9	UV/Vis spectral changes of 1 in a) DMSO (0.53 mM) and b) 50% DMSO/water mixture (0.17 mM) upon incubation in the dark for 16 h.	S17
Figure S10	UV/Vis spectral changes of 1 (0.53 mM) in DMSO upon photolysis at 468 nm with increasing illumination time (0–15 min).	S18
Figure S11	UV/Vis spectral changes of 1 in 50% DMSO/water mixture (0.18 mM) upon incubation in the dark for 16 h in presence of Na ₂ S ₂ O ₄ .	S19
Figure S12	UV/Vis spectral changes in the Q-band of myoglobin (60 μM in 0.1 PBS at pH 7.4) with sodium dithionite (10 mM) and complex 1 (10 μM) under a dinitrogen atmosphere upon incubation in the dark for an hour.	S20
Figure S13	UV/Vis spectral changes of 2 in a) DMSO (0.13 mM) and b) 75% DMSO/water mixture (0.20 mM) upon photolysis at 365 nm with increasing illumination time (0–5 h).	S21
Table S3	Single-crystal X-ray diffraction data of complex 1a .	S22
Figure S14	Half maximal inhibitory concentration values of the title ligand and complexes (1 and 2) against TPH-1 and MB cells, obtained under dark (black curves) and light (blue curves) conditions.	S23

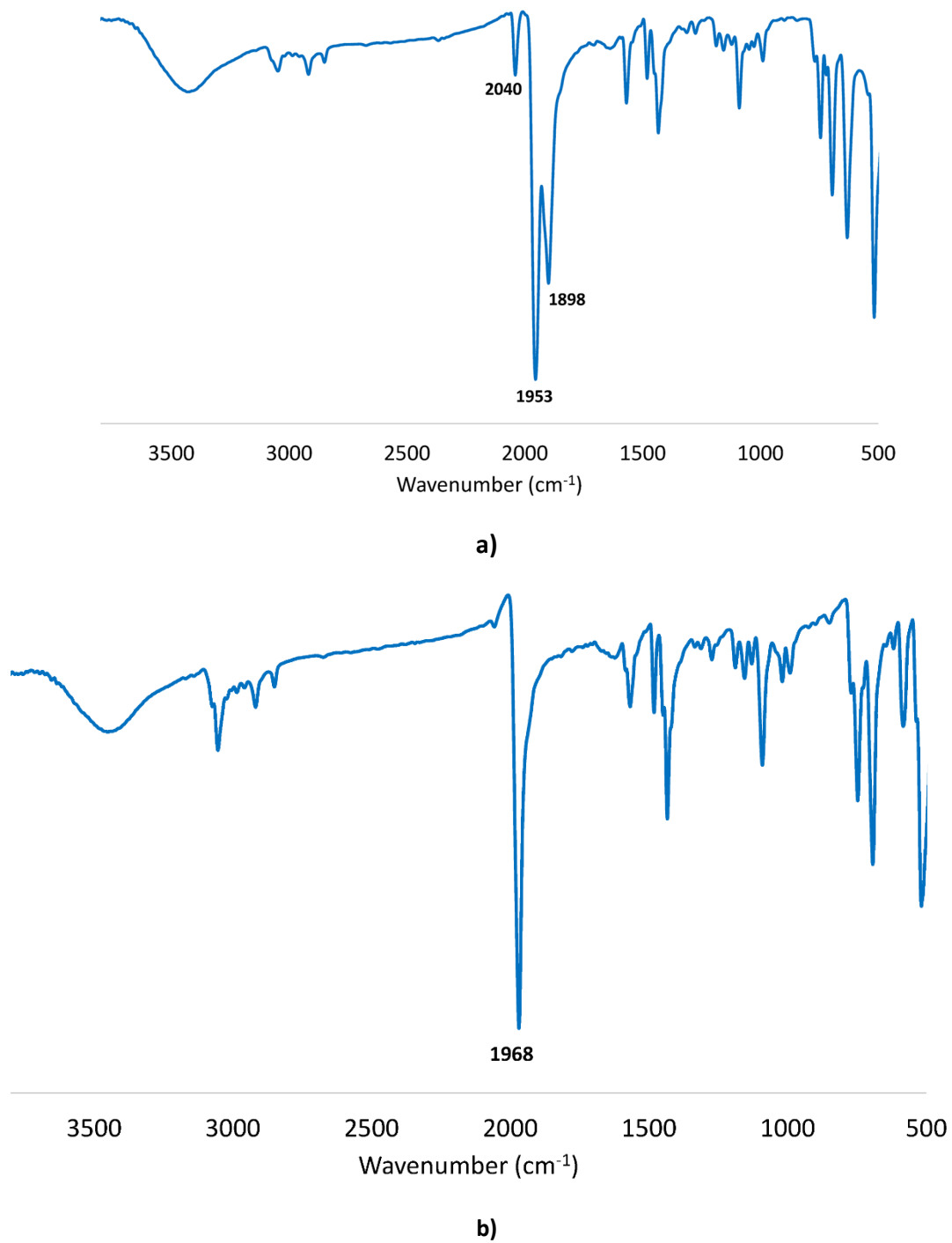


Fig. S1 IR spectra of **a)** $[\text{MnBr}(\text{CO})_2(\kappa^1\text{-P-PPh}_2\text{Py})(\kappa^2\text{-P-N-PPh}_2\text{Py})]$ (**1**) and **b)** $[\text{RuCl}_2(\text{CO})(\kappa^1\text{-P-PPh}_2\text{Py})(\kappa^2\text{-P-N-PPh}_2\text{Py})]$ (**2**).

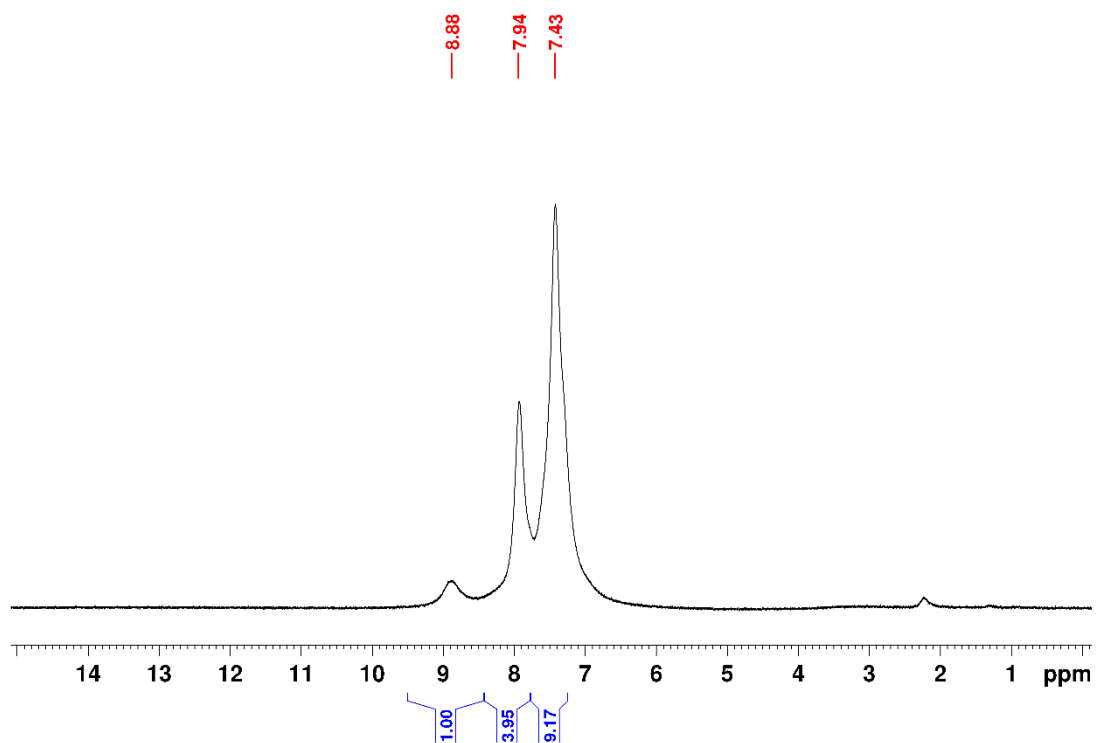


Fig. S2 ^1H NMR spectrum (in CD_3Cl_3) of complex **1**.

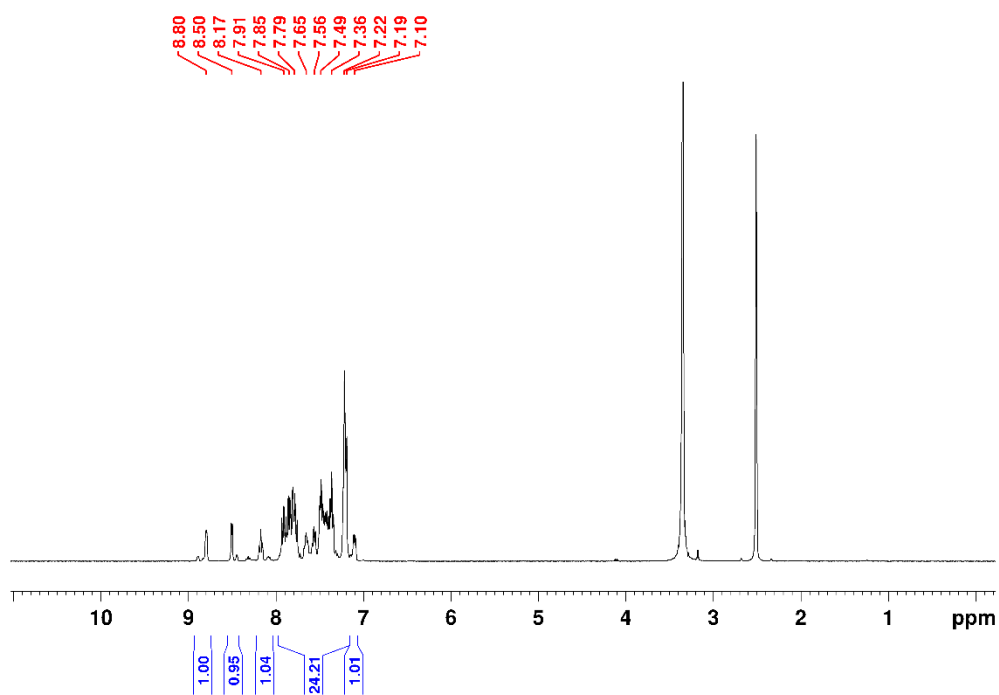


Fig. S3 ^1H NMR spectrum (in DMSO-d_6) of complex **2**.

Table S1 Single-crystal X-ray diffraction data of complex **2**.

Data	2
Empirical formula	C ₃₅ H ₂₈ Cl ₂ N ₂ OP ₂ Ru
Formula weight (g·mol ⁻¹)	726.50
Temperature (K)	100(2)
Radiation, λ (Å)	Cu _{Kα} , 1.54184
Crystal system	monoclinic
Space group	<i>P</i> 2 ₁ / <i>n</i>
<i>Unit cell dimensions</i>	
<i>a</i> (Å)	11.37234(9)
<i>b</i> (Å)	10.76781(8)
<i>c</i> (Å)	25.48891(16)
α (°)	90
β (°)	93.5906(7)
γ (°)	90
Volume (Å ³)	3115.12(4)
<i>Z</i>	4
Calculated density (Mg·m ⁻³)	1.549
Absorption coefficient (mm ⁻¹)	6.877
<i>F</i> (000)	1472
Theta range for collection	3.475 to 75.114°
Reflections collected	64659
Unique reflections	6332
Minimum/maximum transmission	0.318/0.722
Refinement method	Full-matrix least-squares on <i>F</i> ²
Data / parameters / restraints	6332 / 395 / 2
Goodness-of-fit on <i>F</i> ²	1.106
Final <i>R</i> indices [<i>I</i> > 2σ(<i>I</i>)]	<i>R</i> ₁ = 0.0303, <i>wR</i> ₂ = 0.0765
<i>R</i> indices (all data)	<i>R</i> ₁ = 0.0306, <i>wR</i> ₂ = 0.0768
Maximum/minimum residual electron density (e·Å ⁻³)	0.477 / -1.359

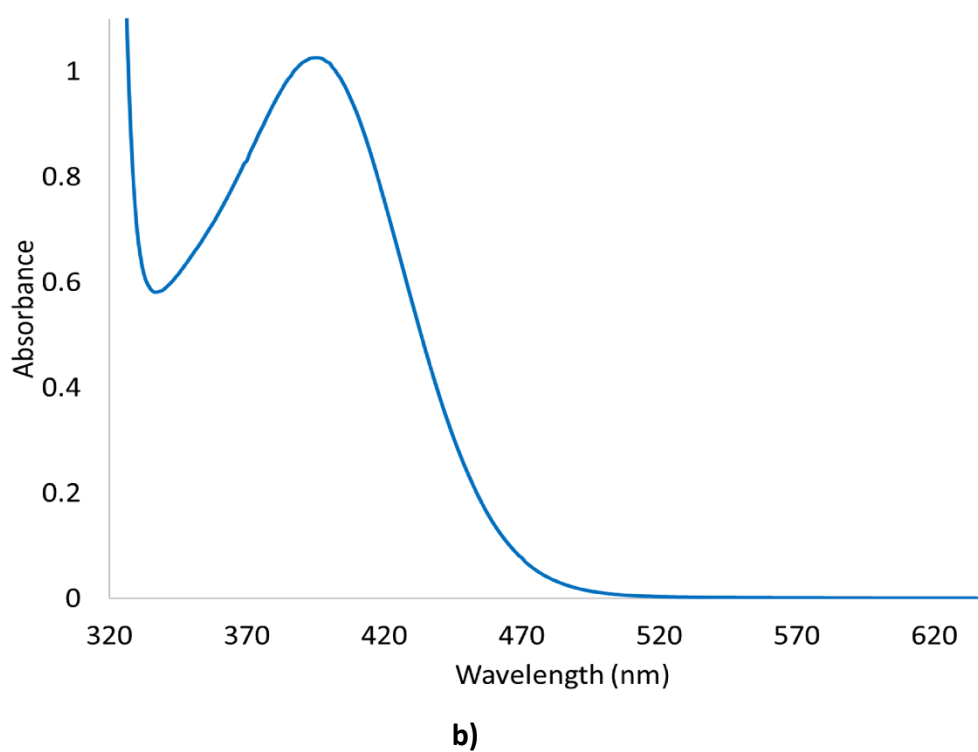
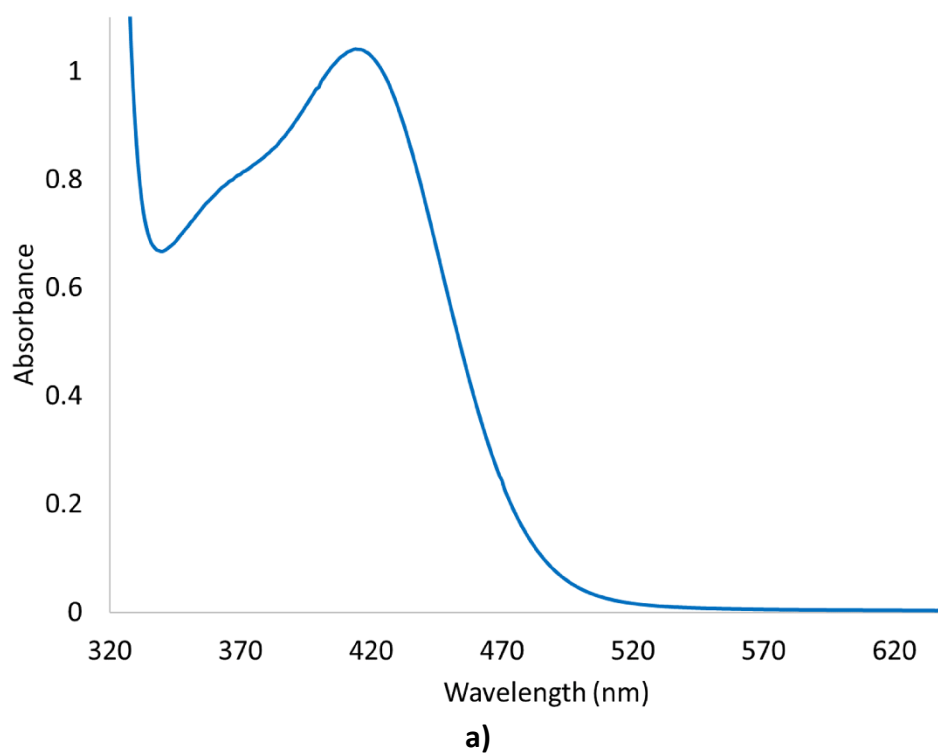


Fig. S4 The electronic absorption spectra of **1** in **a)** DMSO (0.53 mM) and **b)** 50% DMSO/water mixture (0.17 mM).

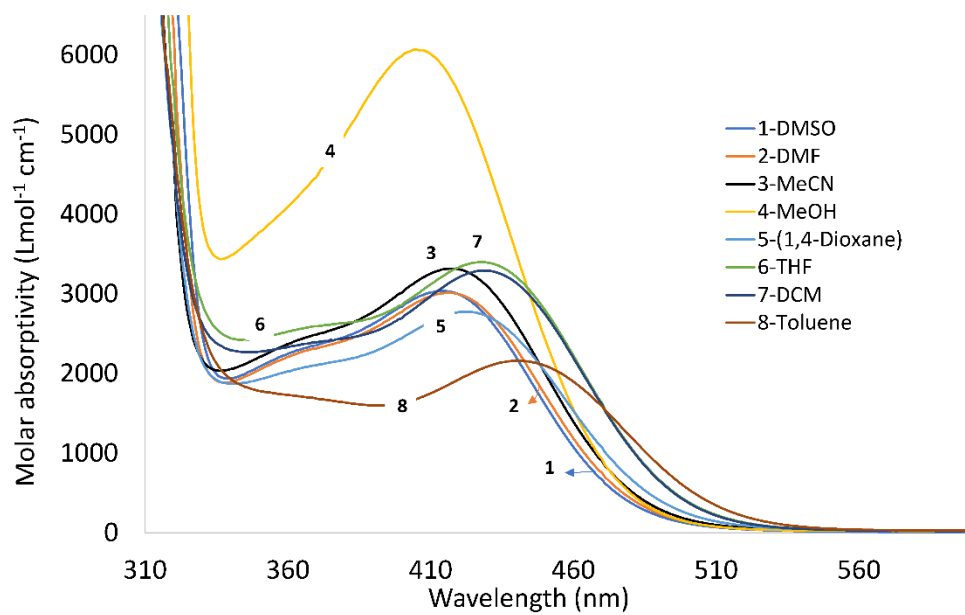
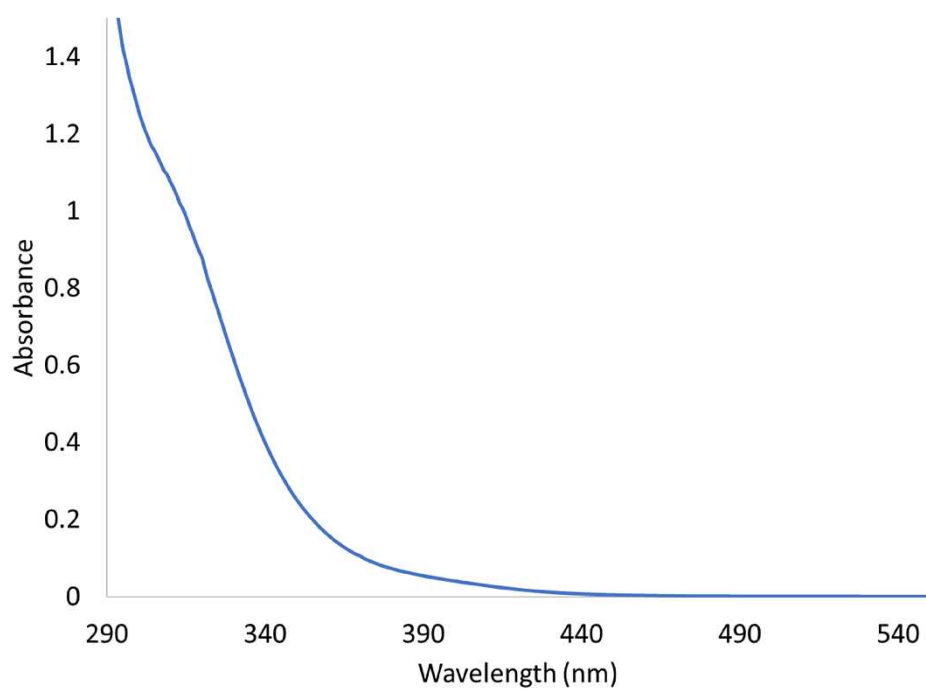


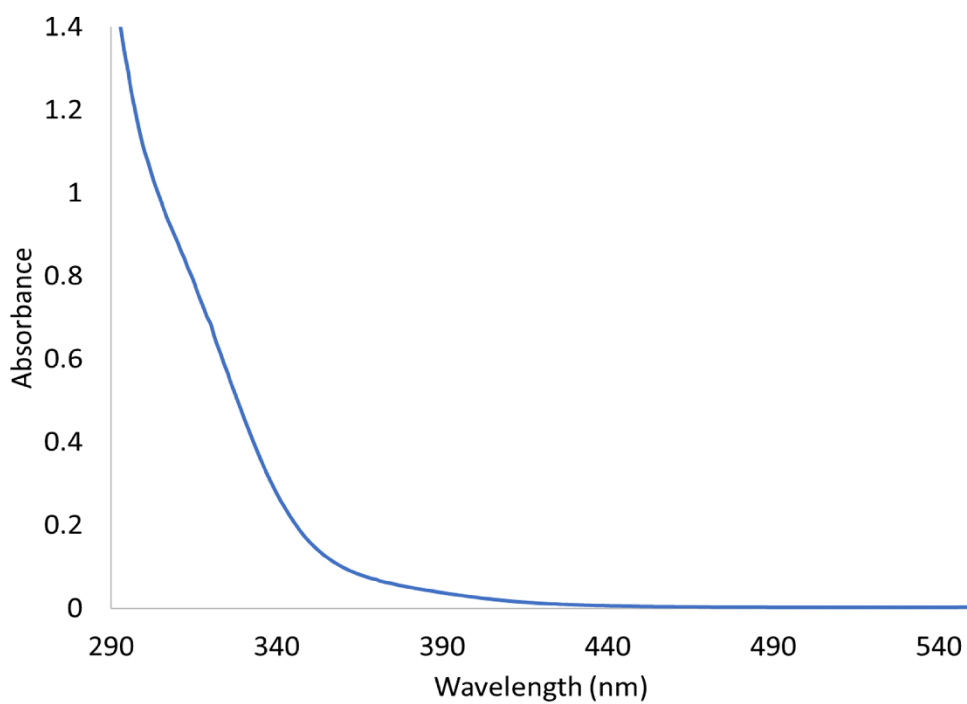
Fig. S5 The electronic absorption spectra of **1** in different solvents showing solvatochromic behaviour.

Table S2 The absorbance maxima (λ_{max} , nm) and molar extinction coefficient of the lowest energy transition of **1** in different solvents.

Solvent	λ_{max} (ϵ_{max})
	1
DMSO	414 nm (3036)
DMF	416 nm (3013)
MeCN	418 nm (3316)
MeOH	405 (6067)
1,4-Dioxane	423 nm (2774)
THF	428 nm (3398)
DCM	428 nm (3291)
Toluene	442 nm (2158)

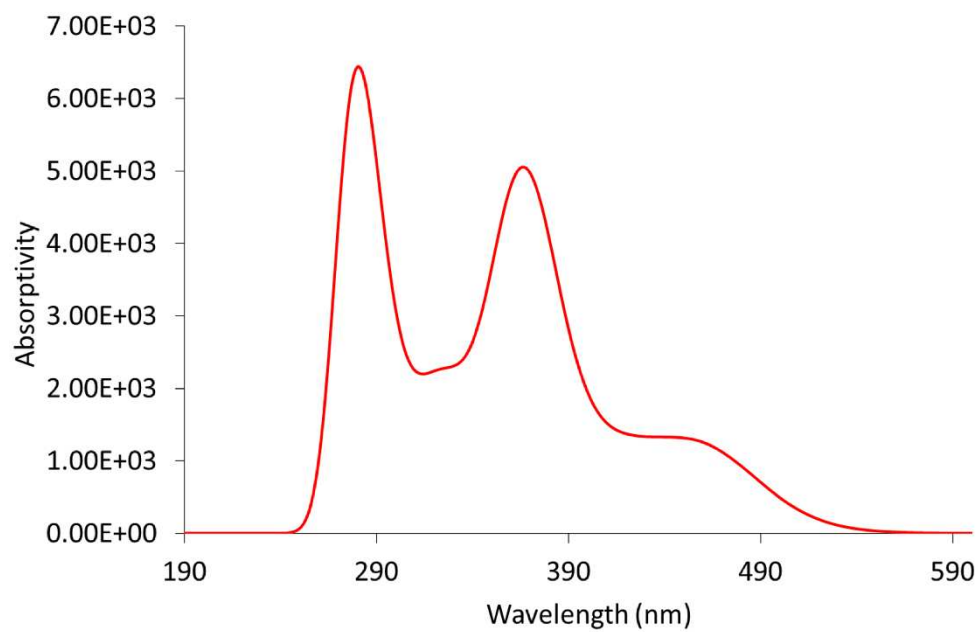


a)

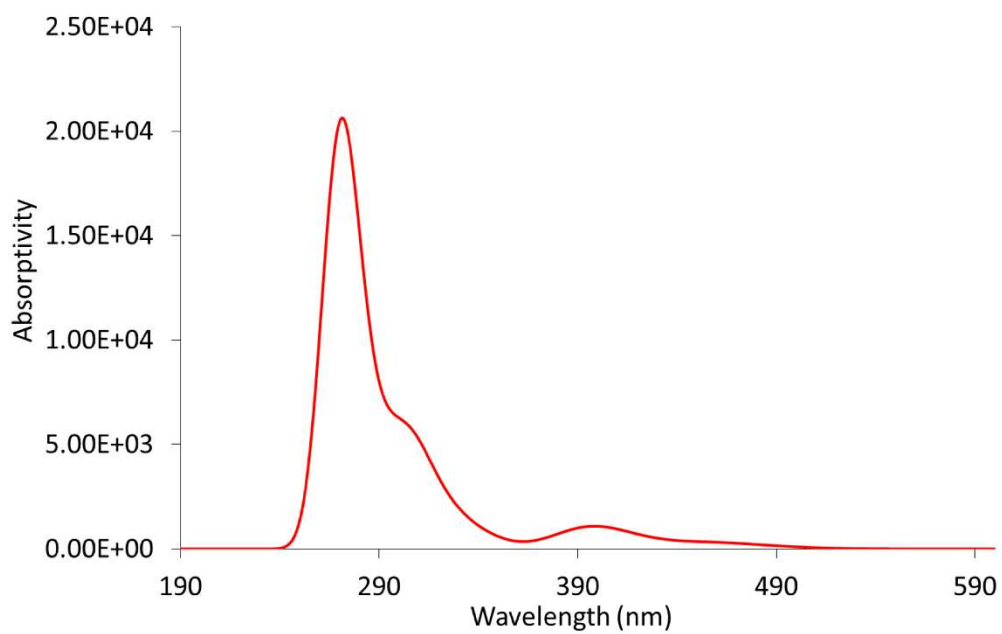


b)

Fig. S6 The electronic absorption spectra of **2** in **a)** DMSO (0.13 mM) and **b)** 75% DMSO/water mixture (0.20 mM).



a)



b)

Fig. S7 TDDFT calculated absorption spectra of **a) 1** and **b) 2**, obtained at B3LYP/LANL2DZ level of theory.

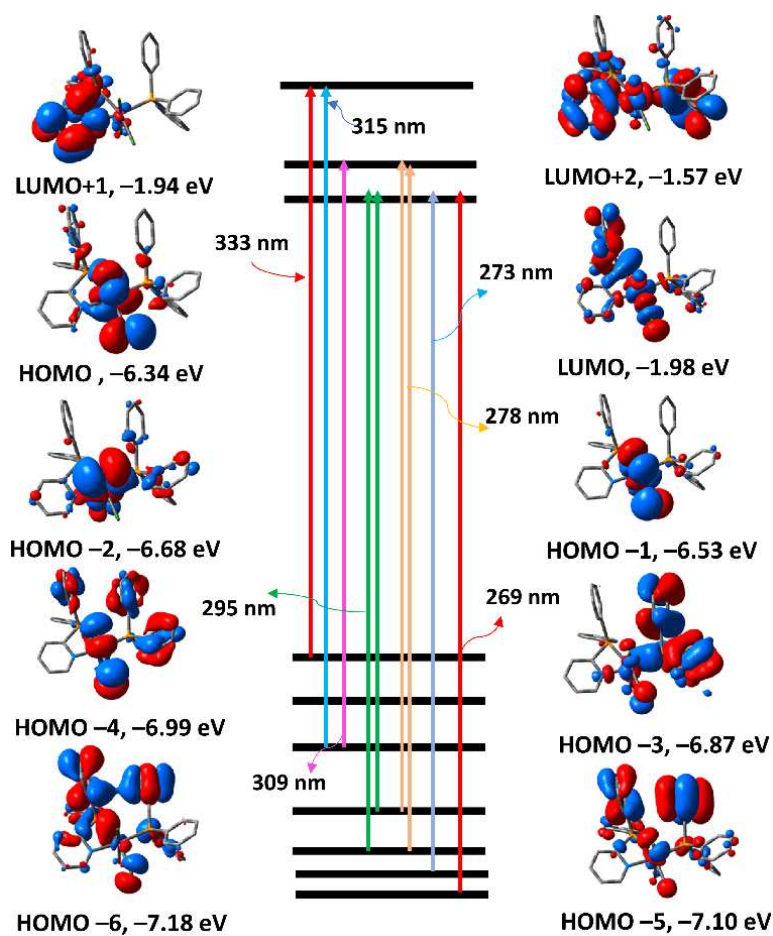
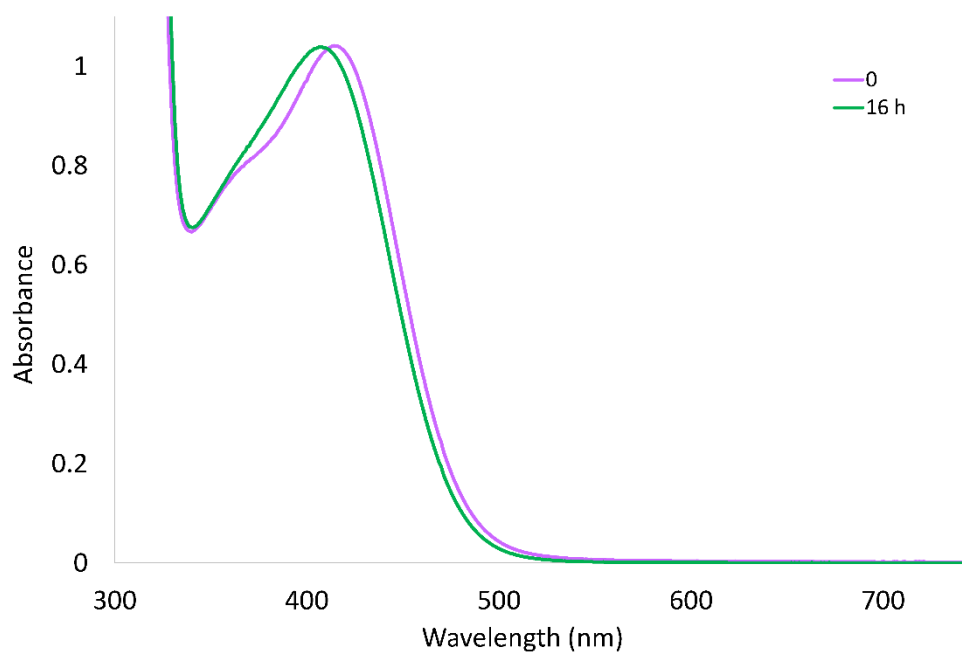
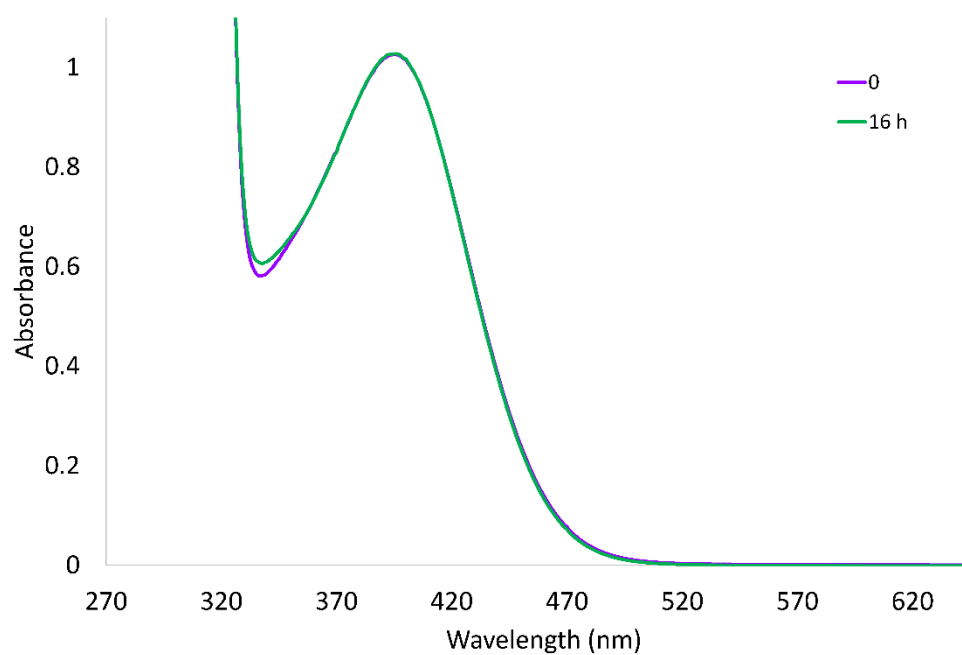


Fig. S8 Selected electronic transitions and Frontier molecular orbitals of complex **2**, calculated at B3LYP/LANL2DZ level of theory.



a)



b)

Fig. S9 UV/Vis spectral changes of **1** in **a)** DMSO (0.53 mM) and **b)** 50% DMSO/water mixture (0.17 mM) upon incubation in the dark for 16 h.

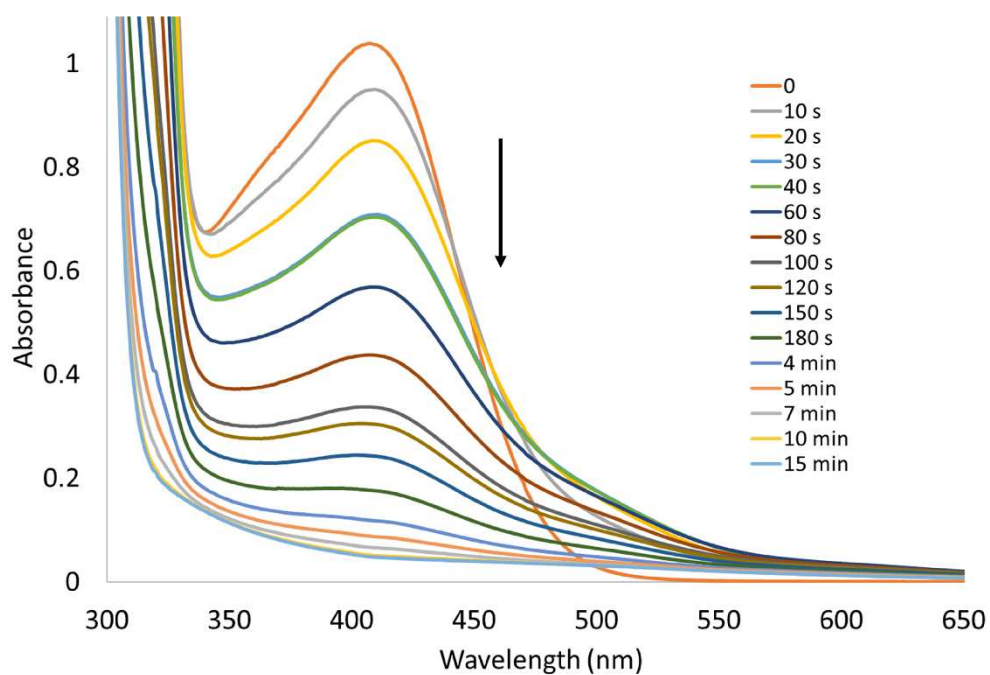


Fig. S10 UV/Vis spectral changes of **1** (0.53 mM) in DMSO upon photolysis at 468 nm with increasing illumination time (0–15 min).

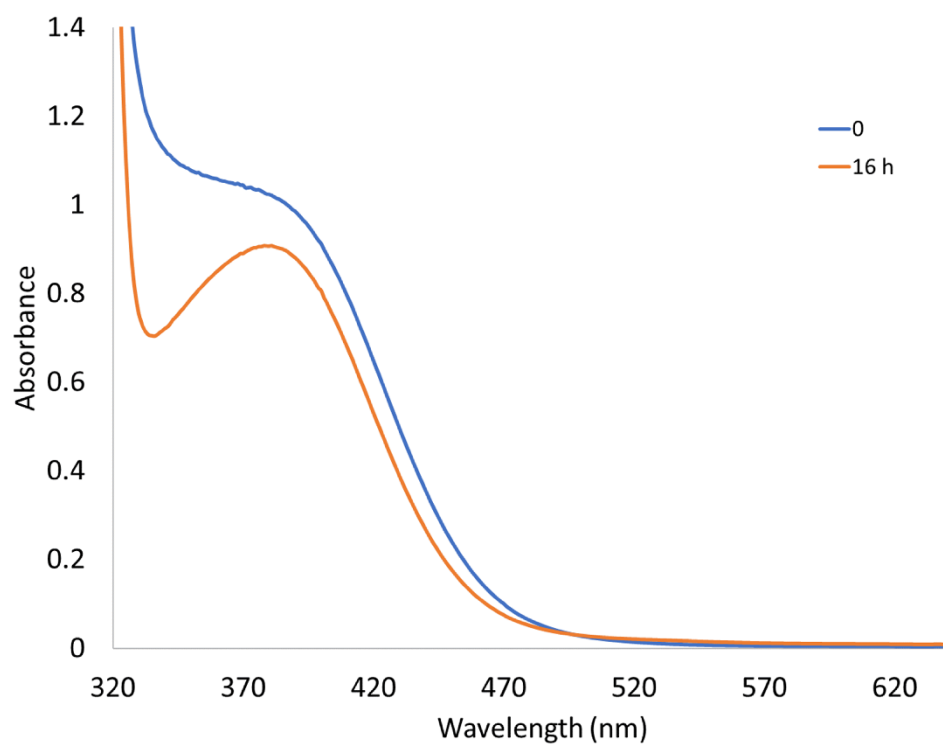


Fig. S11 UV/Vis spectral changes of **1** in 50% DMSO/water mixture (0.18 mM) upon incubation in the dark for 16 h in presence of $\text{Na}_2\text{S}_2\text{O}_4$.

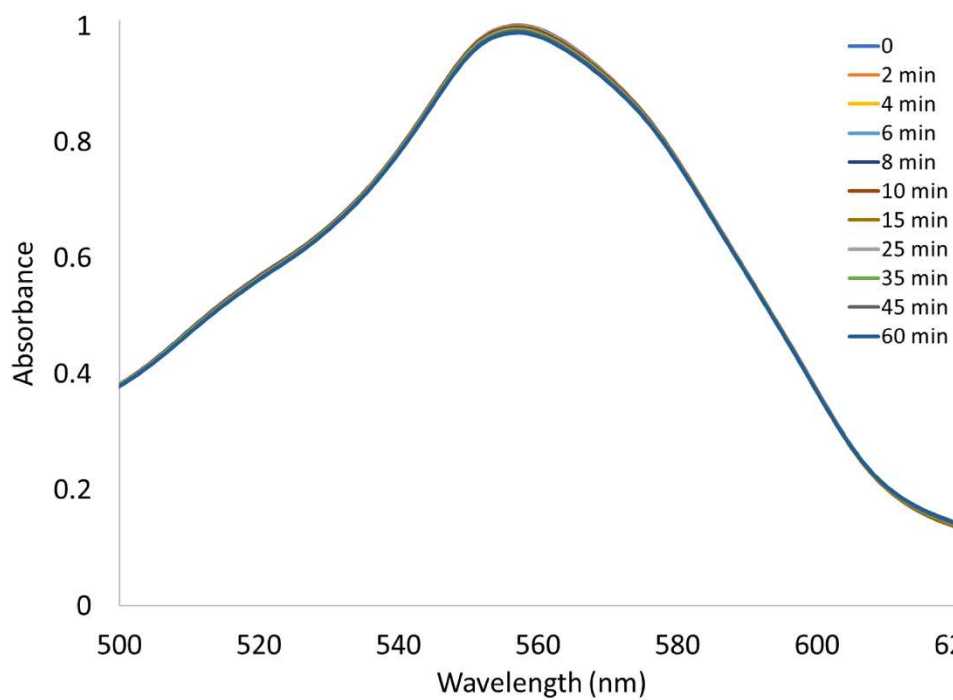
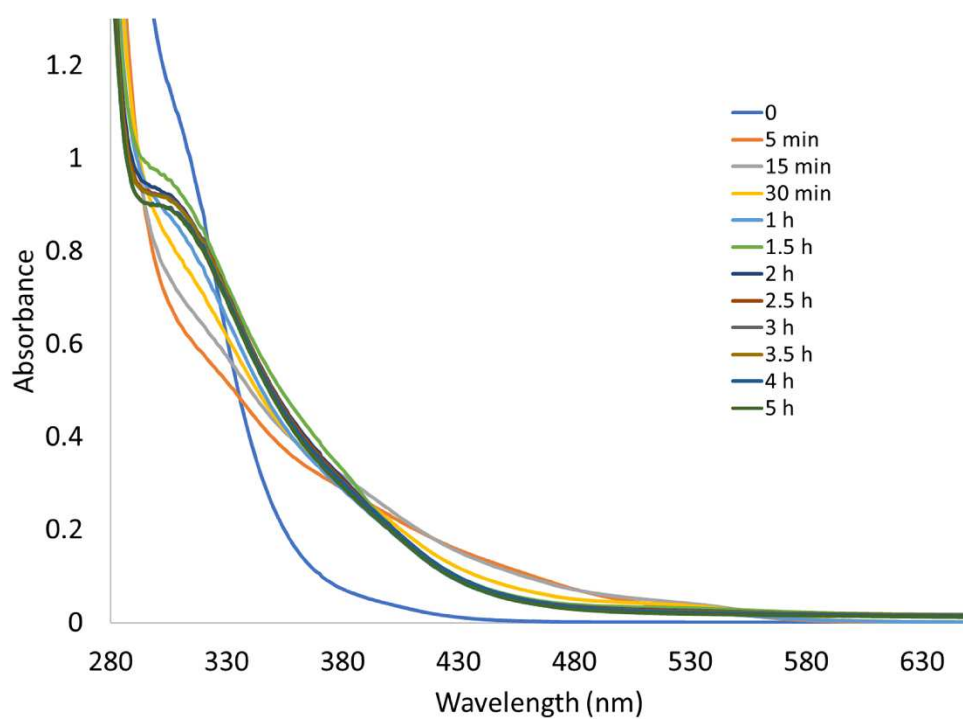
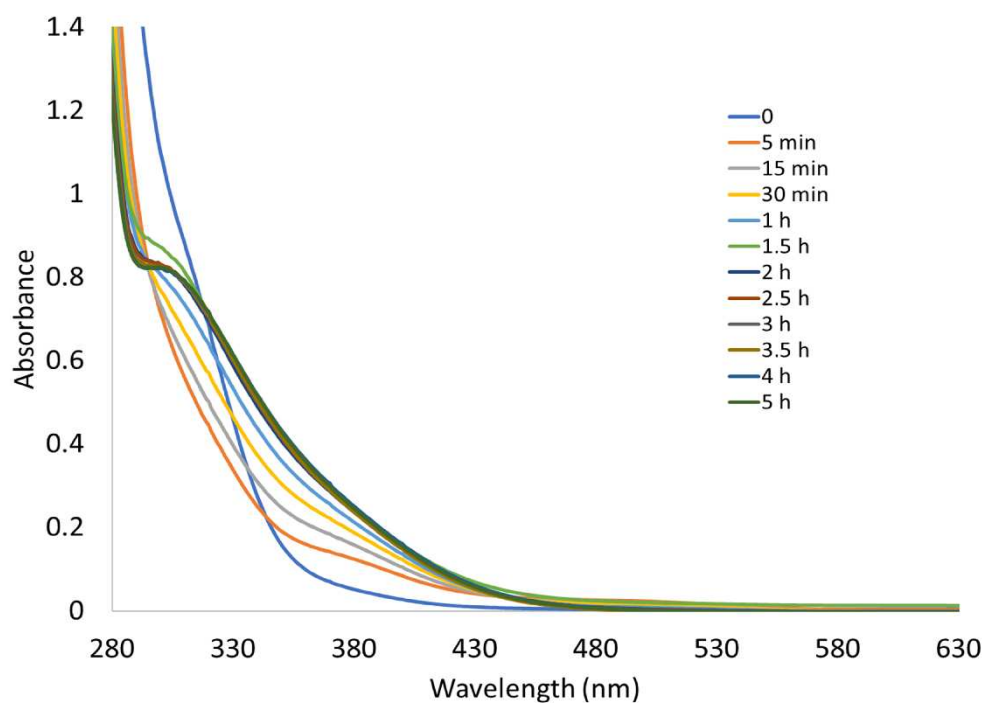


Fig. S12 UV/Vis spectral changes in the Q-band of myoglobin (60 μM in 0.1 PBS at pH 7.4) with sodium dithionite (10 mM) and complex **1** (10 μM) under a dinitrogen atmosphere upon incubation in the dark for an hour.



a)



b)

Fig. S13 UV/Vis spectral changes of **2** in **a)** DMSO (0.13 mM) and **b)** 75% DMSO/water mixture (0.20 mM) upon photolysis at 365 nm with increasing illumination time (0–5 h).

Table S3 Single-crystal X-ray diffraction data of complex **1a**.

Data	1a
Empirical formula	C ₃₄ H ₂₈ Br _{1.30} Cl _{0.70} MnN ₂ O ₂ P ₂
Formula weight (g·mol ⁻¹)	742.34
Temperature (K)	100(2)
Radiation, λ (Å)	Cu _{Kα} , 1.54184
Crystal system	monoclinic
Space group	C2/c
<i>Unit cell dimensions</i>	
<i>a</i> (Å)	21.9592(3)
<i>b</i> (Å)	11.30260(10)
<i>c</i> (Å)	13.1315(2)
α (°)	90
β (°)	101.6700(10)
γ (°)	90
Volume (Å ³)	3191.81(7)
<i>Z</i>	4
Calculated density (Mg·m ⁻³)	1.545
Absorption coefficient (mm ⁻¹)	7.033
<i>F</i> (000)	1498
Theta range for collection	4.419 to 75.152°
Reflections collected	16221
Independent reflections	3210
Minimum/maximum transmission	0.460/0.755
Refinement method	Full-matrix least-squares on <i>F</i> ²
Data / parameters / restraints	3210 / 199 / 0
Goodness-of-fit on <i>F</i> ²	1.055
Final R indices [<i>I</i> >2σ(<i>I</i>)]	<i>R</i> ₁ = 0.0216, <i>wR</i> ₂ = 0.0544
R indices (all data)	<i>R</i> ₁ = 0.0218, <i>wR</i> ₂ = 0.0545
Maximum/minimum residual electron density (e·Å ⁻³)	0.379 / -0.372

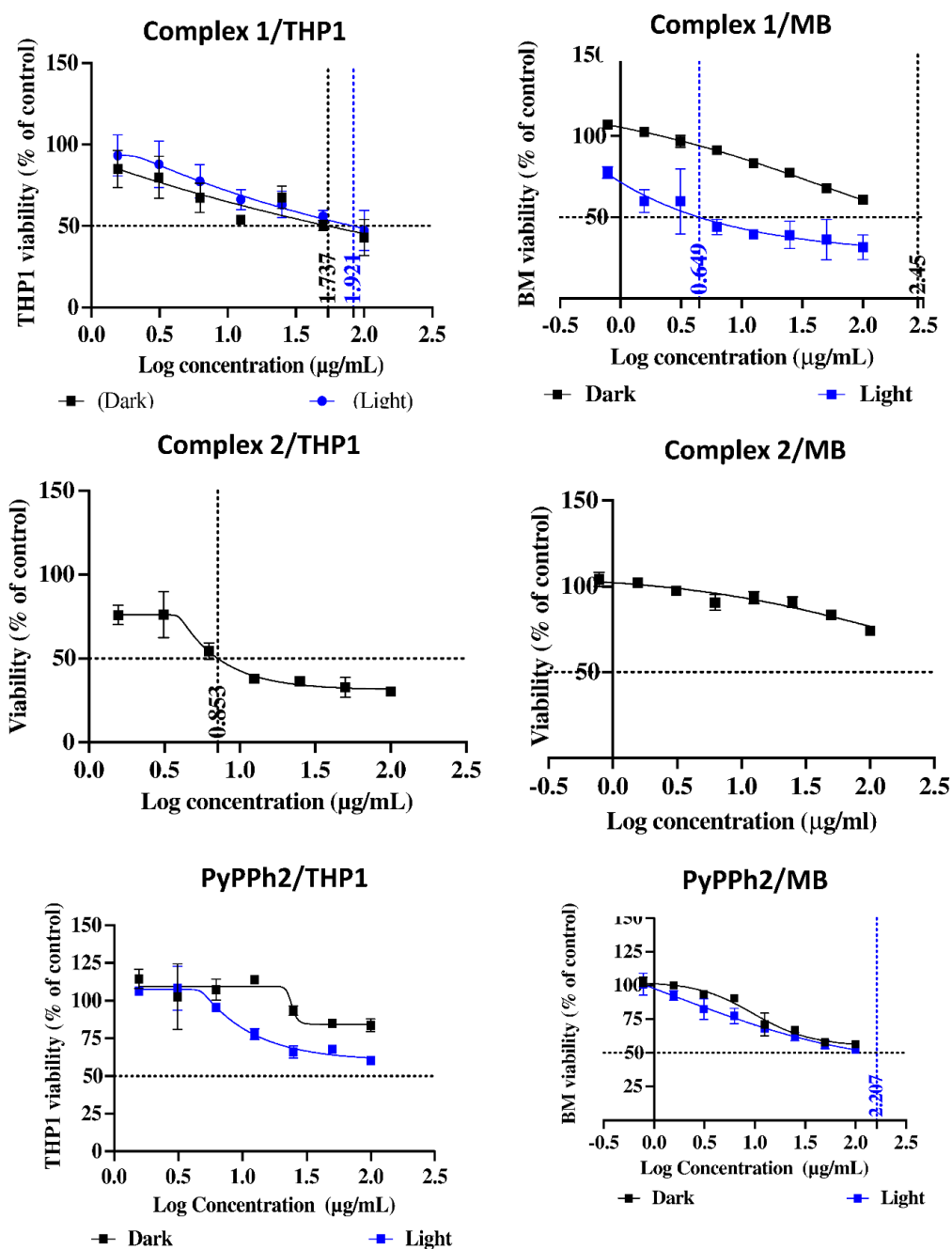


Fig. S14 Half maximal inhibitory concentration values of the title ligand and complexes (**1** and **2**) against TPH-1 and MB cells, obtained under dark (black curves) and light (blue curves) conditions.

References

1. P. A. Anderson, G. B. Deacon, K. H. Haarmann, F. R. Keene, T. J. Meyer, D. A. Reitsma, B. W. Skelton, G. F. Strouse and N. C. Thomas, Designed synthesis of mononuclear tris (heteroleptic) ruthenium complexes containing bidentate polypyridyl ligands, *Inorg. Chem.*, 1995, **34**, 6145-6157.
2. D. A. Habashy, R. M. Khaled, A. Y. Ahmed, K. Radacki, S. K. Ahmed, E. K. Tharwat, H. Magdy, A. Zeinhom and A. M. Mansour, Cytotoxicity of fac-Mn (CO) 3 complexes with a bidentate quinoline ligand towards triple negative breast cancer, *Dalton Trans.*, 2022, **51**, 14041-14048.
3. G. M. Sheldrick, SHELXT—Integrated space-group and crystal-structure determination, *Acta Crystallogr., Sect. A: Found. Adv.*, 2015, **71**, 3-8.
4. G. M. Sheldrick, A short history of SHELX, *Acta Crystallogr., Sect. A: Found. Crystallogr.*, 2008, **64**, 112-122.
5. A. Becke, Density-functional thermochemistry. III. The role of exact exchange (1993) J, *Chem. Phys.*, **98**, 5648.
6. A. D. Becke, Density-functional exchange-energy approximation with correct asymptotic behavior, *Phys. Rev. A*, 1988, **38**, 3098.
7. P. J. Hay and W. R. Wadt, Ab initio effective core potentials for molecular calculations. Potentials for K to Au including the outermost core orbitals, *J. Chem. Phys.*, 1985, **82**, 299-310.
8. P. J. Hay and W. R. Wadt, Ab initio effective core potentials for molecular calculations. Potentials for the transition metal atoms Sc to Hg, *J. Chem. Phys.*, 1985, **82**, 270-283.
9. M. J. Frisch, G. W. Trucks, H. B. Schlegel, G. E. Scuseria, M. A. Robb, J. R. Cheeseman, V. G. Zakrzewski, J. A. Montgomery, J. C. B. R. E. Stratmann, S. Dapprich, J. M. Millam, A. D. Daniels, K. N. Kudin, M. C. Strain, O. Farkas, J. Tomasi, V. Barone, M. Cossi, R. Cammi, B. Mennucci, C. Pomelli, C. Adamo, S. Clifford, J. Ochterski, G. A. Petersson, P. Y. Ayala, Q. Cui, K. Morokuma, D. K. Malick, A. D. Rabuck, K. Raghavachari, J. B. Foresman, J. Cioslowski, J. V. Ortiz, A. G. Baboul, B. B. Stefanov, A. L. G. Liu, I. K. P. Piskorz, R. Gomperts, R. L. Martin, D. J. Fox, T. Keith, M. A. Al-Laham, C. Y. Peng, A. Nanayakkara, C. Gonzalez, M. Challacombe, P. M. W. Gill, B. G. Johnson, W. Chen, M. W. Wong, J. L. Andres, M. Head-Gordon, E. S. Replogle and J. A. Pople, *GAUSSIAN 03 (Revision A.9)*, Gaussian, Inc., Pittsburgh, 2003.
10. A. Frisch, A. B. Nielson and A. J. Holder, Gaussview User Manual, *Gaussian, Inc., Pittsburgh, PA*, 2000, .
11. S. McLean, B. E. Mann and R. K. Poole, Sulfite species enhance carbon monoxide release from CO-releasing molecules: implications for the deoxy-myoglobin assay of activity, *Analytical biochemistry*, 2012, **427**, 36-40.
12. A. J. Atkin, J. M. Lynam, B. E. Moulton, P. Sawle, R. Motterlini, N. M. Boyle, M. T. Pryce and I. J. Fairlamb, Modification of the deoxy-myoglobin/carbonmonoxy-myoglobin UV-vis assay for reliable determination of CO-release rates from organometallic carbonyl complexes, *Dalton Trans.*, 2011, **40**, 5755-5761.
13. D. E. Maridas, E. Rendina-Ruedy, P. T. Le and C. J. Rosen, Isolation, culture, and differentiation of bone marrow stromal cells and osteoclast progenitors from mice, *J. Visualized Exp.*, 2018, e56750.
14. M. B. Hansen, S. E. Nielsen and K. Berg, Re-examination and further development of a precise and rapid dye method for measuring cell growth/cell kill, *J. Immunol. Methods*, 1989, **119**, 203-210.